AD-A261 859

REPORT DOCUMENTATION PAGE

Form Approved
OBM No. 0704-0188

Report Date. 1993

3. Report Type and Dates Covered. Final - Proceedings

4. Title and Subtitle.
The Use of Spectral Decomposition in Determining the Plane Wave Spectrum of the Incident Acoustic Field on a Rough Sea Surface

5. Funding Numbers.
Contract
Program Element No. 0602435N
Project No. 03526
Task No. JOV
Accession No. DN250019
Work Unit No. 12211K

6. Author(s).
Guy V. Norton and Richard S. Keiffer

7. Performing Organization Name(s) and Address(es).
Naval Research Laboratory
Ocean Acoustics Directorate
Stennis Space Center, MS 39529-5004

8. Performing Organization Report Number.
PR 91:135:221

9. Sponsoring/Monitoring Agency Name(s) and Address(es).
Naval Research Laboratory
Exploratory Development Program Group
Stennis Space Center, MS 39529-5004

10. Sponsoring/Monitoring Agency Report Number.
PR 91:135:221

11. Supplementary Notes.
Published in IMACS, Computational Acoustics.

12a. Distribution/Availability Statement.
Approved for public release; distribution is unlimited.

12b. Distribution Code.

13. Abstract *(Maximum 200 words).*

One hybrid approach to studying the effects of scattering from a rough sea surface on acoustic transmission in a waveguide makes use of a description of the incident acoustic field in terms of its plane wave spectrum (PWS). This is a convenient form because many scattering models assume plane wave incidence. In this paper, an expression for the PWS of the acoustic field incident on a flat sea surface is developed from a spectral decomposition of the depth coordinate operator and a source term provided by a finite element parabolic equation (FEPE) model (1). Previously, the spectral decomposition method was used to couple the scattering from a spherical target in free space to an ocean waveguide. (2) Details of the coupling between the propagation and scattering model are presented. A numerical experiment is considered in which the PWS is used to develop input to a wedge assemblage (WA) scattering model (3-5) in order to simulate a canonical one convergence zone backscatter experiment.

14. Subject Terms.
Underwater acoustics, active acoustic propagation, surface scattering, ambient noise

15. Number of Pages. 12

16. Price Code.

17. Security Classification of Report.	18. Security Classification of This Page.	19. Security Classification of Abstract.	20. Limitation of Abstract.
Unclassified	Unclassified	Unclassified	SAR

NSN 7540-01-280-5500

Standard Form 298 (Rev. 2-89)
Prescribed by ANSI Std. Z39-18
298-102

REPRINTED FROM

Computational Acoustics

Acoustic Propagation

Proceedings of the 3rd IMACS Symposium on
Computational Acoustics
Cambridge, MA, USA, 26-28 June, 1991

Volume 2

edited by

Ding LEE
Naval Undersea Warfare Center
New London, Connecticut
U.S.A.

Robert VICHNEVETSKY
Department of Computer Science
Rutgers University
New Brunswick, New Jersey
U.S.A.

Allan R. ROBINSON
Division of Applied Sciences
Harvard University
Cambridge, Massachusetts
U.S.A.

N·H

1993

NORTH-HOLLAND
AMSTERDAM • LONDON • NEW YORK • TOKYO

Computational Acoustics - Volume 2
D. Lee, A.R. Robinson and R. Vichnevetsky (Editors)
Elsevier Science Publishers B.V. (North-Holland)
1993 IMACS

The Use of Spectral Decomposition in Determining the Plane Wave Spectrum of the Incident Acoustic Field on a Rough Sea Surface

Guy V. Norton and Richard S. Keiffer
Naval Oceanographic and Atmospheric Research Laboratory
Acoustic Theory and Simulation Branch
Stennis Space Center, Mississippi 39529-5004

Abstract: One hybrid approach to studying the effects of scattering from a rough sea surface on acoustic transmission in a waveguide makes use of a description of the incident acoustic field in terms of its plane wave spectrum (PWS). This is a convenient form because many scattering models assume plane wave incidence. In this paper, an expression for the PWS of the acoustic field incident on a flat sea surface is developed from a spectral decomposition of the depth coordinate operator [$Q = \rho\frac{\partial}{\partial z}\rho^{-1}\frac{\partial}{\partial z} + k^2(r,z)$] and a source term provided by a finite element parabolic equation (FEPE) model [1]. Previously, the spectral decomposition method was used to couple the scattering from a spherical target in free space to an ocean waveguide [2]. Details of the coupling between the propagation and scattering model are presented. A numerical experiment is considered in which the PWS is used to develop input to a wedge assemblage (WA) scattering model [3-5] in order to simulate a canonical one convergence zone backscatter experiment.

1. INTRODUCTION

Acoustic propagation models have generally been developed with the assumption that the air-water interface (sea-surface) is flat and that the pressure-release boundary conditions prevail on this boundary. On the other hand, scattering models generally assume that the propagating medium is a homogeneous halfspace. It seems appropriate to attempt to marry these two efforts in order to develop a hybrid approach aimed at better simulating acoustic transmission though an ocean waveguide with a rough upper boundary. This paper will describe a general approach to such a hybrid model that, specifically, is used to couple a propagation model (Parabolic Equation model) with a WA scattering model.

Generally speaking, models for the scattering from a rough sea surface require that the incident field on the surface be specified in some form and, of course, that some description of the surface roughness or its statistics be known. A convenient form to specify the incident field is in terms of it's PWS (i.e., the magnitude and phase of the collection of plane waves that define the incident field). This is so because many scattering models

assume plane wave incidence and point sources can always be placed sufficiently far away to achieve this effect.

In mode theory, assuming a layered medium, one can determine the horizontal eigenvalues of the propagating or discrete modes, and associate with each mode (in each layer) an angle of propagation. The problem with using mode theory to determine the PWS is that there is a significant computational burden associated with calculating the strength of each mode. In addition most normal mode programs handle range dependency by requiring that range dependent properties change in an adiabatic manner. A better technique would be to allow an accurate range-dependent acoustic propagation model to determine the propagated acoustic field and then use this field to determine the field incident on the sea surface in terms of its PWS.

We present the following coupling scheme. First propagate the acoustic signal in the waveguide using a Parabolic Equation (PE) based model, (in our case, FEPE). At the range of interest, take a vertical section of the field throughout the depth of the waveguide. Spectrally decompose the depth coordinate operator associated with the PE equation, taking the vertical field as the source term so as to obtain the eigenvalues and the magnitude of each mode in the layer (isovelocity assumed) just below the air-water interface. Use this information (the spectral decomposition function), to develop the PWS and feed this information into the WA scattering model, which can determine the scattered field in either the forward, backward or out of plane directions. Use this model (which assumes a homogeneous halfspace) to determine the scattered field in depth. Use this vertical field as the new source term in the spectral decomposition model in order to incorporate it properly in the waveguide. Finally use this scattered field to properly perturb the incident field, and propagate this new field in the waveguide. Once the spectral decomposition functions are found, they need not be found again until the environment in which it was solved changes.

We will not present in detail the theory behind the PE model or the WA scattering model. We will, however, include the necessary background information to properly follow the paper. First we present the some background information on the WA scattering model. Next we present the theory behind spectral decomposition along with describing how this method is used to developed the necessary inputs to the WA scattering model. We next spectrally decompose the depth operator for a typical deep water environment. After obtaining the PWS at the sea surface, we use this information as input into the WA scattering model to determine the resulting back scattered field in depth. This field is then propagated back to the source.

2. THE WEDGE ASSEMBLAGE SCATTERING MODEL

Briefly, the building block of the WA scattering model [3-5] is the Biot and Tolstoy (B-T) exact solution [6] for the acoustic impulse response of an infinite, impenetrable wedge. The solution applies for arbitrarily located point sources and receivers and all wedge angles. A unique feature of this solution is that it provides a time domain picture of the scattered wave that has two time-separable parts: a delta function arrival due to reflections

from any properly oriented wedge faces and a diffracted pressure wave due to the wedge apex. Both the B-T solution and the WA approach have successfully compared against experimental data.

As it applies to 1-D or long-crested surfaces like the one to be considered later, the WA method of calculating the scattering from rough surfaces essentially consists of modeling the surface of interest with an assemblage of rectangular facets (any cojoint facet faces define a wedge) and numerically evaluating the B-T solution for each wedge in the assemblage. It should be noted that for the backscattering geometries of relevance to this study, reflections from facet faces are either unlikely or weak (or both). Thus, each evaluation of the B-T solution results only in a time series for the diffracted wave. The impulse response of the entire surface is then taken to be the sum, with due respect to individual arrival times, of all the individual responses; an FFT is generally performed on this time series to provide the scattered response for particular frequencies.

3. SPECTRAL DECOMPOSITION

The following discussion closely follows the work presented by Gilbert and Evans [7], and Gilbert and Di [2], although we use cubic Hermite basis functions as opposed to "hat" functions used by the previous authors. We start with the expression for the acoustic pressure P in an azimuthally symmetric, depth dependent sound speed and density ocean waveguide,

$$\frac{\partial^2 P}{\partial r^2} + \frac{1}{4}\frac{\partial P}{\partial r} + \rho\left(\frac{\partial}{\partial z}\right)\rho^{-1}\left(\frac{\partial}{\partial z}\right)P + k^2(r,z)P = 0. \tag{3.1}$$

where k is the wavenumber, ρ is the density of the fluid while r and z are the range and depth coordinate respectively. We introduce the following variable $\Psi = \sqrt{r}\,P$ and upon substitution we obtain for a far field expression

$$\frac{\partial^2 \Psi}{\partial r^2} + \rho\left(\frac{\partial}{\partial z}\right)\rho^{-1}\left(\frac{\partial}{\partial z}\right)\Psi + k^2(r,z)\Psi = 0. \tag{3.2}$$

Rewriting the above equation as a product of operators,

$$\left(\frac{\partial}{\partial r} + i\sqrt{Q}\right)\left(\frac{\partial}{\partial r} - i\sqrt{Q}\right)\Psi = 0 \tag{3.3}$$

where $Q = \rho\frac{\partial}{\partial z}\rho^{-1}\frac{\partial}{\partial z} + k^2(r,z)$. Formally solving for $\partial\Psi/\partial r$ gives

$$\frac{\partial \Psi}{\partial r} = \pm\, i\,\sqrt{Q}\,\Psi. \tag{3.4}$$

We are interested only in out going waves, therefore we chose $+i\sqrt{Q}$. Solving for Ψ gives,

$$\Psi(r,z) = e^{i\Delta r\sqrt{Q}}\,\Psi(r_0,z) \tag{3.5}$$

where $\Delta r = r - r_o$. We now need to obtain an explicit solution from Eq. (3.5) for Ψ. In order to do this we use the spectral representation for a function of an Operator Q.

$$F(Q) = \frac{1}{2\pi i} \oint \frac{F(x)}{xI - Q} dx \tag{3.6}$$

where I is the unit operator, $1/(xI-Q)$ represents the inverse of xI-Q and the limits of integration are over the entire spectrum of Q. Using Eq. (3.6) with Eq. (3.5) and defining x $= \kappa^2$, where κ is the horizontal wavenumber and $dx = 2\kappa d\kappa$, we obtain

$$\Psi(r,z) = \frac{1}{\pi i} \oint \frac{e^{i\Delta r\kappa}}{\kappa^2 I - Q} \Psi(r_o,z)\kappa d\kappa. \tag{3.7}$$

Suppressing the unit operator and defining

$$\frac{1}{\kappa^2 - Q} \Psi(r_o,z) \equiv \Phi(\kappa,r_o,z) \tag{3.8}$$

or

$$(Q - \kappa^2)\, \Phi(\kappa,r_o,z) = -\Psi(r_o,z) \tag{3.9}$$

We now write the z dependence explicitly in a slightly different form as,

$$\left(\frac{\partial^2}{\partial z^2} + \frac{1}{\rho}\frac{\partial \rho}{\partial z}\frac{\partial}{\partial z} + \frac{\omega^2}{c^2} - \kappa^2\right)\Phi(\kappa,r_o,z) = -\Psi(r_o,z) \tag{3.10}$$

where ω is the angular frequency, c is the local sound speed which in general is both depth and range dependent. Equation (3.7) is used in order to reconstruct the total field, and can be rewritten as the following,

$$\Psi(r,z) = \frac{1}{\pi i} \oint e^{i\Delta r\kappa}\, \Phi(\kappa,r_o,z)\kappa d\kappa. \tag{3.11}$$

4. NUMERICAL SOLUTION

4.1 Galerkin Method

The following procedure is described in great detail by Sewell [8]. We use the Galerkin method to solve the partial differential equation, Eq. (3.10). Equation (3.10) along with the boundary conditions at the surface and the bottom describe a steady state boundary value problem. The boundary conditions are

$\Phi(\kappa,r_o,z = 0) = 0$ at the beginning of the interval R, designated as $\partial R_1 = \{z = 0\}$

$\Phi(\kappa,r_o,z = Zmax) = 0$ at the end of the interval R, designated as $\partial R_2 = \{z = Zmax\}$

where R is the interval [0, Zmax]. Recasting Eq. (3.10) into a more compact form

$$\Phi''(\kappa,r_o,z) + \left(\frac{1}{\rho}\right)\rho'\Phi'(\kappa,r_o,z) + \frac{\omega^2}{c^2}\Phi(\kappa,r_o,z) - \kappa^2\Phi(\kappa,r_o,z) + \Psi(r_o,z) = 0 \tag{4.1}$$

where the primes indicate the partial derivative with respect to z. Multiplying Eq. (4.1) by a smooth function, $\chi(z)$, that vanishes on $\partial R_1 = \{z = 0, Zmax\}$ and integrating over [0,Zmax] gives

$$0 = \int_0^{Zmax} \left\{ \Phi'' + \left(\frac{1}{\rho}\right) \rho' \Phi' + \frac{\omega^2}{c^2} \Phi - \kappa^2 \Phi + \Psi \right\} \chi dz. \tag{4.2}$$

Integrating by parts and realizing that, $\chi(0) = \chi(Zmax) = 0$, we obtain

$$0 = \int_0^{Zmax} \left\{ -\Phi'\chi' + \left(\frac{1}{\rho}\right) \rho' \Phi' \chi + \frac{\omega^2}{c^2} \Phi \chi - \kappa^2 \Phi \chi + \Psi \chi \right\} dz. \tag{4.3}$$

Now Eq. (4.3) is almost equivalent to Eq. (4.1) in that if Φ is smooth and satisfies Eq. (4.3) for any smooth χ vanishing at ∂R_1 and ∂R_2 the steps leading from Eq. (4.1) to Eq. (4.3) can be reversed, so that Φ satisfies Eq. (4.1) and the natural boundary conditions at z=Zmax and Φ must satisfy the first (essential) boundary condition. The solution to Eq. (4.3) will have the following form

$$\Phi(\kappa, r_o, z) = \Omega(\kappa, r_o, z) + \sum_{i=1}^{M} a_i \chi_i (\kappa, r_o, z) \tag{4.4}$$

where $\{\chi_1, \ldots, \chi_M\}$ is a set of linearly independent "trial" function that vanish at ∂R_1 and Ω is another function that satisfies the essential boundary condition $\Omega = 0$ at ∂R_1. It is required that Eq. (4.3) be satisfied for $\chi = \chi_1, \ldots, \chi_m$ each vanishing at ∂R_1:

$$\int_0^{Zmax} \left\{ -\Phi'\chi'_k + \left(\frac{1}{\rho}\right) \rho' \Phi' \chi_k + \frac{\omega^2}{c^2} \Phi \chi_k - \kappa^2 \Phi \chi_k + \Psi \chi_k \right\} dz = 0. \tag{4.5}$$

This can be written as a system of M linear equations for M unknown parameters

$a_1, \ldots a_M$.;

$$\sum_{i=1}^{M} A_{ki} a_i = b_k \tag{4.6}$$

where

$$b_k = \int_0^{Zmax} \left[\Psi \chi_k - \Omega' \chi'_k + \frac{1}{\rho} \rho' \Omega' \chi_k + \frac{\omega^2}{c^2} \Omega \chi_k - \kappa^2 \Omega \chi_k \right] dz, \tag{4.7}$$

$$A_{ki} = \int_0^{Zmax} \left[\chi'_k \chi'_i - \frac{1}{\rho} \rho' \chi_k \chi'_i - \frac{\omega^2}{c^2} \chi_k \chi_i + \kappa^2 \chi_k \chi_i \right] dz. \tag{4.8}$$

The essential boundary conditions are satisfied automatically by the proper choice of basis functions. We choose the function Ω to equal zero and the function $\chi_1, \ldots \chi_m$ was chosen from the "cubic Hermite" basis functions, defined by

$$H_k(z) = 3\left[\frac{z-z_{k-1}}{k_k-z_{k-1}}\right]^2 - 2\left[\frac{z-z_{k-1}}{k_k-z_{k-1}}\right]^3 \quad \text{for } z_{k-1} \le z \le z_k$$

$$= 3\left[\frac{z_{k+1}-z}{k_{k+1}-z_k}\right]^2 - 2\left[\frac{z_{k+1}}{k_{k+1}-z_k}\right]^2 \quad \text{for } z_k \le z \le z_{k+1}$$

$$= 0 \quad \text{elsewhere,} \tag{4.9}$$

and

$$S_k(z) = \frac{(z-z_{k-1})^2}{(k_k-z_{k-1})} + \frac{(z-z_{k-1})^3}{(k_k-z_{k-1})^2} \quad \text{for } z_{k-1} \le z \le z_k$$

$$= \frac{(z_{k+1}-z)^2}{(k_{k+1}-z_k)} - \frac{(z_{k+1}-z)^3}{(k_{k+1}-z_k)^2} \quad \text{for } z_k \le z \le z_{k+1}$$

$$= 0 \quad \text{elsewhere,} \tag{4.10}$$

where $z_{-1} < 0 = z_0 < z_1 < \ldots < z_M = Zmax < z_{M+1}$. These functions are piecewise cubic polynomials and are constructed so that they and their first derivatives are continuous. The trial function is given as the following,

$$\{\chi_1, \ldots \chi_{2N+1}\} = \{S_0, H_1, S_1, \ldots H_N, S_N\} \tag{4.11}$$

so the number of unknowns and equations is M=2N+1. The function Ω satisfies the boundary conditions at ∂R_1 and ∂R_2 and each χ_k vanishes at both end points, so they are acceptable trial functions.

Using the cubic Hermite basis functions specified above, the matrix A is banded with half-bandwidth equal to 3. The integral in Eqs. (4.7) and (4.8) were evaluated numerically using Gauss's 3 point rule, which is exact for polynomials of degree 5. The nodes were spaced uniformly, $z_j = j\Delta z$ ($\Delta z = Zmax/N$).

5. DETERMINING THE PWS

The expression developed here for the PWS incident on a particular patch of the ocean surface from the spectral decomposition of the depth coordinate operator is analogous to one developed earlier based from normal mode theory for a layered waveguide [9]. Therefore, it is appropriate to revisit the pertinent concepts of normal mode theory. It is well known that in such an environment the acoustic field can be determined via a sum of normal modes,

$$P(r,z) = C \sum_m \Phi(\gamma_m z_s)\, \Phi(\gamma_m z) \frac{e^{i\kappa_m r}}{\sqrt{\kappa_m r}} \tag{5.1}$$

where Φ is the vertical eigenfunction, γ and κ are the vertical and horizontal eigenvalues respectively and r is the horizontal range from the source to the receiver, z_s is the source depth and z is the depth of the receiver. The depth eigenfunction can be described as follows,

$$\Phi(\gamma_{mz}) = A_m \sin(\gamma_m z) + B_m \cos(\gamma_m z), \tag{5.2}$$

where A_m and B_m are mode and depth dependent coefficients. Considering the top layer of the waveguide, the coefficient B_m vanishes in order to satisfy the upper boundary condition. Eq. (5.1) now becomes,

$$P(r,z) = C \sum_m \Phi(\gamma_m z_s)\, A_m \sin(\gamma_m z) \frac{e^{i\kappa_m r}}{\sqrt{\kappa_m r}} \tag{5.3}$$

which, expanding the sine in terms of exponentials, gives

$$P(r,z) = C \sum_m \Phi(\gamma_m z_s)\, A_m \frac{e^{i(\kappa_m r+\gamma_m z)} - e^{i(\kappa_m r-\gamma_m z)}}{2i\sqrt{\kappa_m r}}\,. \tag{5.4}$$

Note that in the top layer the sum over normal modes is now expressed in terms of a sum over up and down going plane waves. To obtain the field incident upon the sea surface (which is assumed flat), the down going plane waves are dropped, leaving an expression which when evaluated at z=0 is the incident field on the flat sea surface.

$$P_{inc}(r,z{=}0) = C \sum_m \Phi(\gamma_m z_s)\, A_m \frac{e^{i\kappa_m r}}{2i\sqrt{\kappa_m r}} = \sum_m \Pi_m\,. \tag{5.5}$$

The grazing angle of each plane wave is given by $\theta_m = \arccos(\kappa_m \cdot c1/\omega)$, where c1 is the sound speed in the top isovelocity layer. Note that because of the pressure-release boundary condition at the sea surface, dropping the up-going plane waves from Eq. (5.4) and evaluating the result at z=0 would have resulted in a reflected field and PWS that, as expected for flat pressure-release surface, differs only in sign from Eq. (5.5).

Now, following a similar line of thought, but starting from Eq. (3.11). Equating Eq. (3.11) to Eq. (5.4):

$$\frac{1}{\pi i} \oint e^{i\Delta r\kappa}\Phi(\kappa,r_o,z)\ \kappa d\kappa = C \sum_m \varphi(\gamma_m z_s)\ A_m \sin(\gamma_m z)\frac{e^{i\kappa_m r}}{\sqrt{\kappa_m}} \tag{5.6}$$

and solving for Π_m as in Eq. (5.5) yields

$$\frac{1}{\pi i} \oint e^{i\Delta r\kappa}\Phi(\kappa,r_o,z)\ \kappa d\kappa = 2i\sqrt{r} \sum_m \Pi_m \sin(\gamma_m z) \tag{5.7}$$

$$\frac{-1}{2\pi} \oint \frac{e^{i\kappa\Delta r}\Phi(\kappa,r_o,z)\ \kappa d\kappa}{\sin(\gamma z)} = \sum_m \Pi_m \tag{5.8}$$

The expression for the incident field becomes

$$P_{inc}(r,z\rightarrow 0) = \frac{-1}{2\pi\sqrt{r}} \oint \frac{e^{i\kappa\Delta r}\Phi(\kappa,r_o,z)\ \kappa d\kappa}{\sin(\gamma z)}. \tag{5.9}$$

Equation (5.9) provides the PWS in terms of the spectral decomposition function. A few words about the behavior of Eq. (5.9) is in order. Due to the surface boundary condition which requires that the acoustic pressure goes to zero at the surface, the spectral decomposition function $\Phi(\kappa,r_o,z)$ will go to zero when z=0. However, the combination of $\frac{\Phi(\kappa,r_o,z)}{\sin(\gamma z)}$ remains nearly constant in the top isovelocity layer as z goes to zero. This fact enables Eq. (5.9) to be evaluated at depths approaching zero, or approaching the surface from the underneath side.

6. NUMERICAL EXAMPLE

In this section, a numerical experiment is described that aims at being illustrative and of some practical interest. To those ends, the techniques developed in this paper are applied to the problem of analyzing the backscattering from a rough sea surface one convergence zone away from the source. In order to keep the problem relatively simple, the otherwise flat

sea surface in the area of the convergence zone has been replace by a simple wedge-like deformation of the pressure-release surface. Therefore, there is no back or forward scattering in this experiment except for what is due to this wedge-like surface perturbation.

The waveguide in this experiment, is a typical deep water environment, see Fig. 1. A source frequency of 250 Hz, results in approximately 246 modes. The source depth is 212 m. Figure 2 illustrates the acoustic field expressed as transmission loss as predicted by a normal mode model. Note that between approximately 23 and 38 km there appears to be high-angle energy incident upon the surface and a convergence zone begins at approximately 40 km.

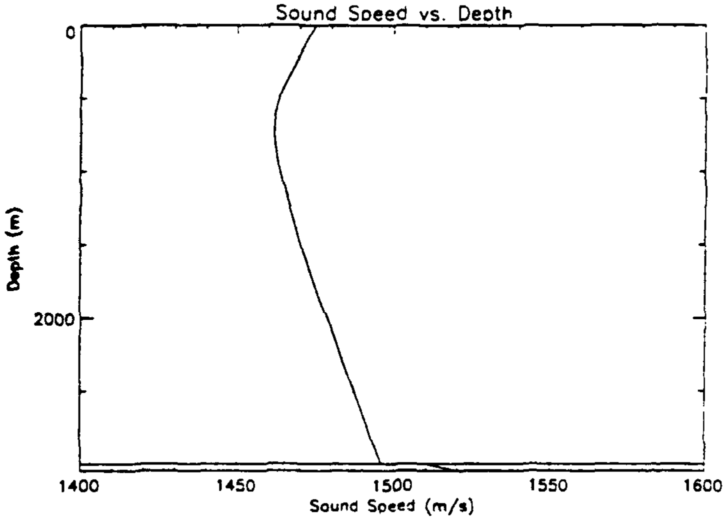

Fig. 1. Sound speed profile used in numerical experiment.

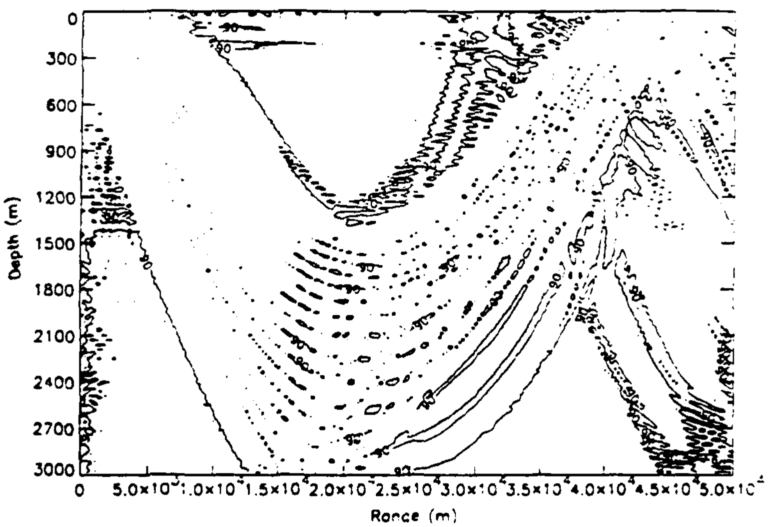

Fig. 2. Transmission loss (dB re 1m) field plot, (90 dB contour shown).

Before developing the PWS we must demonstrate that the propagated field as determined by Eq. (3.11) agrees with the FEPE result. This capability is essential if we are to be successful in determining the PWS, since Eq. (3.11) is the basis for determining the PWS. We used a vertically distributed complex acoustic field that was determined by the FEPE propagation model at a range of 5000 m from the source. This was the source term in Eq. (3.10). Once the spectral decomposition function was determined for a specific depth, the total field Ψ was reconstructed in range using Eq. (3.11). The integration was performed by using an alternating extended Simpson's rule. Before discussing the results a brief discussion on the integration contour is in order.

The integral of Eq. (3.11) stipulates that the integration limits must be over the complete wavenumber spectrum. The branch cuts used were the same as those used by Gilbert and Di [2]. There are two branch cuts, one above and one below the real axis. The lower branch cut returns essentially the discrete contributions while the top branch cut returns essentially the continuous contributions. It appears that as long as the two cuts enclose the discrete spectrum and a portion of the continuous spectrum the results obtained are quite good. Fig. 3 shows the magnitude of the spectral decomposition function vs. horizontal wavenumber for the two branch cuts. Figure 3a is for the lower cut providing the contribution of the discrete spectrum while Fig 3b is the upper cut providing the contribution of the continuous spectrum. Figure 4 compares the output of Eq. (3.11), 4a, to the FEPE output, 4b, for a depth of 4 m. The comparison is very good, thus indicating that the limits of the integration (0.68, 1.08) were adequate to describe the incident field.

We now determine the PWS of the incident field upon the sea surface. Figure 5 compares the PWS as determined by Eq. (5.9) to that produced by Eq. (5.5). The field produced by the spectral decomposition theory Eq. (5.9) is offset by 10 dB so as to allow a better comparison of the two methods. Notice that in both cases the convergence zone is well defined and in general the comparison is quite good. The next step was to place a wedge at a range of 40 km from the source and to determine the PWS at that range incident on the wedge. Figure 6 illustrates geometry of the wedge as well as the placement of the receiver array. Once the PWS was determined, it was used as input into the WA scattering model.

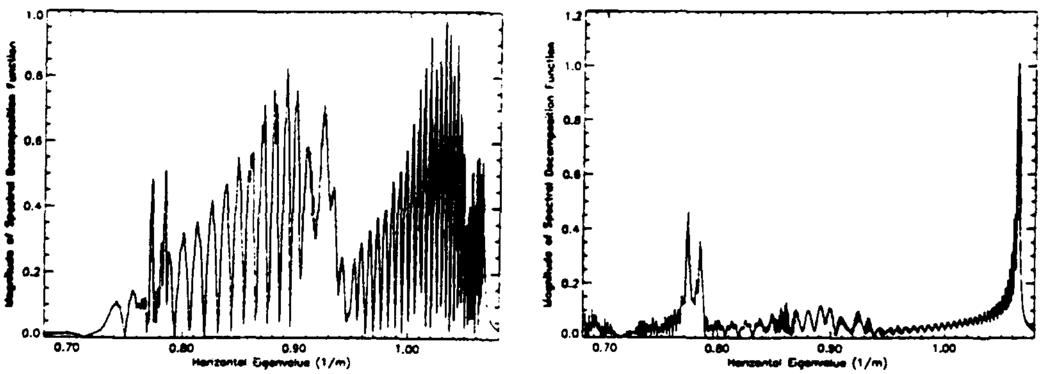

3a. 3b.

Fig. 3. Magnitude of spectral decomposition function vs. horizontal eigenvalue for 3a) lower branch cut, 3b) upper branch cut.

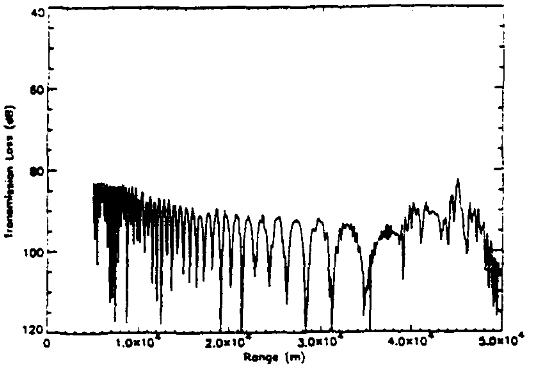

4a.

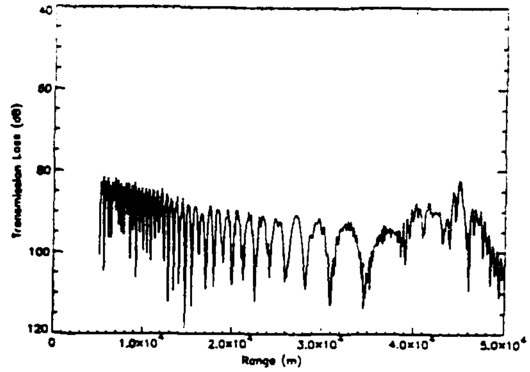

4b.

Fig. 4. Transmission Loss (dB re 1m) vs. range using,
4a) spectral decomposition method Eq. (3.11) and 4b) the FEPE model.

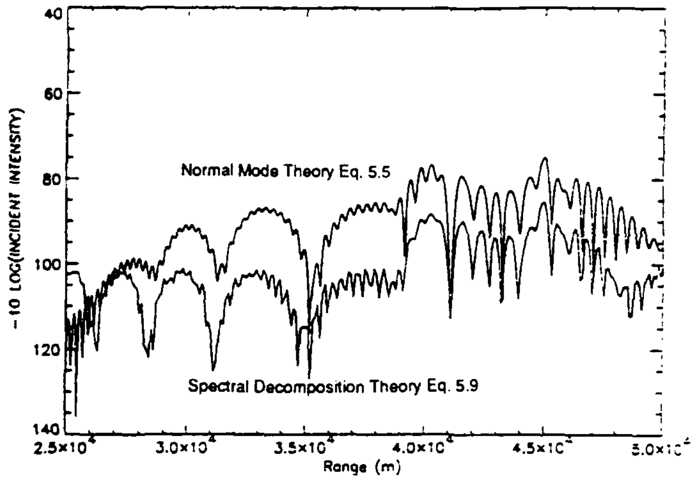

Fig. 5. Comparison of normal mode theory and spectral decomposition theory for determining the PWS.

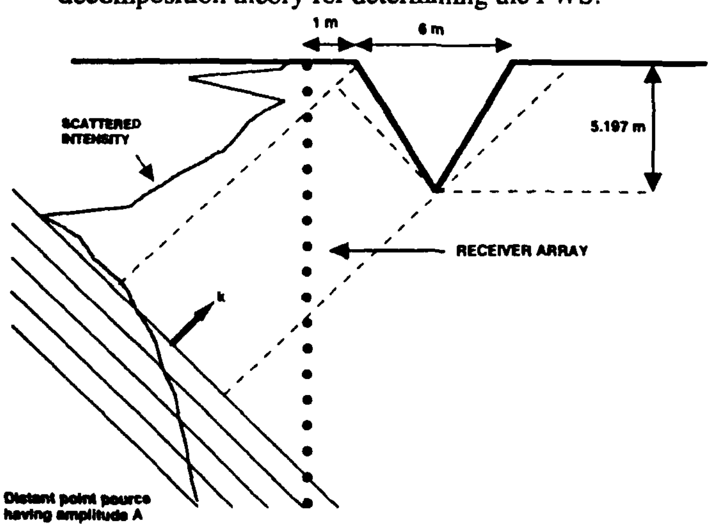

Fig. 6. The geometry for the numerical experiment, showing the wedge and the receiver array.

The resulting scattered field was determined in depth, at a range of 1 m from the wedge, Fig. 7 illustrates the field. The field has a maximum at a depth of 10 m. The field diminishes quite rapidly in depth. This field was used as the source term of Eq. (3.10) and the spectral decomposition function was determined. Using the same limits of integration ($0.68\ m^{-1}$, $1.08\ m^{-1}$) as before, Eq. (3.11) was used to recon-struct the total field in depth since the original scattered field, (Fig. 7) lacked waveguide effects. Figure 8 shows the results. It should be noted that expanded limits of integration ($0.25\ m^{-1}$, $1.25\ m^{-1}$ yielded the same vertical pressure field. Notice that the field again has a peak at a depth of approximately 10 m. The field still diminishes quite rapidly, but now there appears to be an oscillatory pattern to the field. In general there appears to be an overall smoothing to the original field. This field was used to start the FEPE model and propagated back to the source. Figure 9 depicts the resulting field plot. The field is quite small, over 60 dB smaller than the incident field. There appears to be two lobes of energy, one which insonifies the bottom and the other which travels along the convergence zone path back to the source.

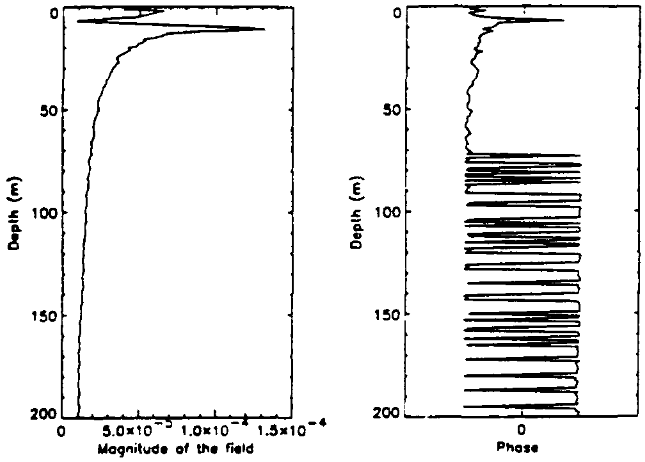

Fig. 7. The magnitude and phase vs. depth of the scattered field as determined by the WA scattering model.

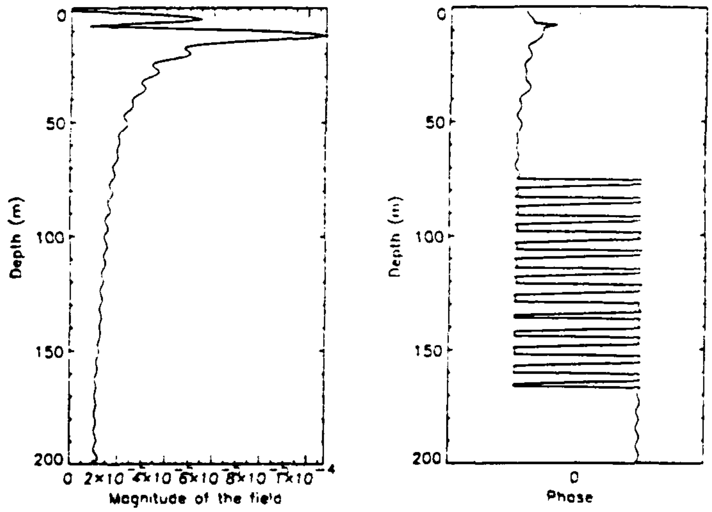

Fig. 8. The magnitude and phase vs. depth of the scattered field after being incorporated in the waveguide via Eq. (3.11).

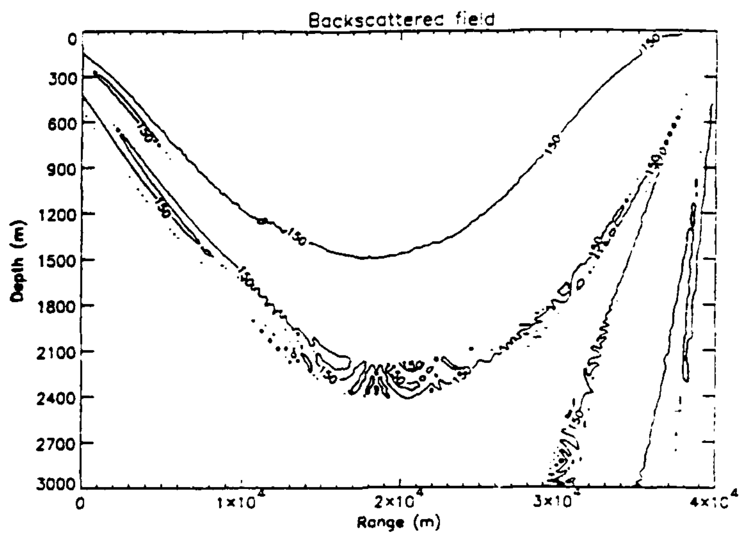

Fig. 9. Transmission loss (dB re 1m) field plot of the backscatteredfield propagated back to the receiver. (Wedge is at 40 km and receiver is at 0 km.)

7. SUMMARY

A method of determining the PWS of the incident acoustic field on a rough surface using spectral decomposition was discussed, details on the approach were provided. The PWS was used as input to the WA scattering model. The WA scattering model generated the scattered field vs. depth, 1m in range from a wedge placed at the ocean surface. This vertical field was then used as a source in the waveguide and propagated back to the receiver.

A major drawback to this technique is that the present numerical implementation of this method is computationally intensive. Methods of overcoming this problem are being investigated. The example given was range independent, however there is no limitation on this method that requires the environment to be so.

ACKNOWLEDGMENTS

This work has been supported by the Office of Naval Technology. The authors would like to thank Dr. Dan Purrington for many helpful and enriching discussions.

REFERENCES

[1] M. D. Collins, "Applications and time-domain solution of higher-order parabolic equations in underwater acoustics," J. Acoust. Soc. Am., 1989, 86, 1097.

[2] Kenneth E. Gilbert and Xiao Di, " Spectral decomposition and propagation of scattered fields in an ocean waveguide," in Computational Acoustics-Vol. 2, edited by D. Lee, A. Cakmak, and R. Vichnevetsky, North-Holland, IMACS 1990, pp 49-63.

[3] Richard S. Keiffer and Novarini, J. C., "A wedge assemblage method for 3-D acoustic scattering from sea surfaces: comparison with a Helmholtz-Kirchoff method," in Computational Acoustics-Vol. 1, edited by D. Lee, A. Cakmak and R. Vichnevetsky, North-Holland, IMACS 1990, pp 67-81.

[4] Medwin, H. and Novarini, J. C., "Backscattering strength and the range dependence of sound scattered from the ocean surface," *J. Acoust. Soc. Am.*, 1981, 69, 108.

[5] Kinney, W. A., Clay, C. S., and Sandness, G. A., "Scattering from a corrugated surface: Comparison between experiment Helmholtz-Kirchoff theory and the facet ensemble method," *J. Acoust. Soc. Am.* 1983, 73, 183.

[6] Biot, M. A. and Tolstoy, I., "Formulation of wave propagation in infinite media by normal coordinates with application to diffraction," *J. Acoust. Soc. Am.*, 1957, 29, 381.

[7] Gilbert, K. E. and Evans, R. B., "A Greens function method for one-way propagation in a range-dependent ocean environment," Ocean Seismo-Acoustics, edited by T. Akal and J. M. Berkson, NATO Conference Series, Series IV: Marine Sciences, 16, Plenum Press, New York, 1986.

[8] Sewell, Granville, "The numerical solution of ordinary and partial differential equations," Harcourt Brace Jovanovich, Publishers, Academic Press, 1988.

[9] Keiffer, R. S. and Norton, G. V., "An approximate technique for extracting the surface reflected plane wave spectrum from certain acoustic propagation models," 8th International Conference on Mathematical and Computer Modeling, 1-4 April, 1991.